Homology-based functional proteomics by mass spectrometry: Application to the *Xenopus* microtubule-associated proteome

Adam J. Liska[1]**[†], Andrei V. Popov[2]*[†], Shamil Sunyaev[3], Peg Coughlin[4], Bianca Habermann[5], Anna Shevchenko[1], Peer Bork[2], Eric Karsenti[2] and Andrej Shevchenko[1]

[1]Max Planck Institute of Molecular Cell Biology and Genetics, Dresden, Germany
[2]European Molecular Biology Laboratory, Heidelberg, Germany
[3]Genetics Division, Department of Medicine, Brigham & Women's Hospital and Harvard Medical School, Boston, MA 02115
[4]Department of Cell Biology, Harvard Medical School, Boston, MA, USA
[5]Scionics, Dresden, Germany

The application of functional proteomics to important model organisms with unsequenced genomes is restricted because of the limited ability to identify proteins by conventional mass spectrometry (MS) methods. Here we applied MS and sequence-similarity database searching strategies to characterize the *Xenopus laevis* microtubule-associated proteome. We identified over 40 unique, and many novel, microtubule-bound proteins, as well as two macromolecular protein complexes involved in protein translation. This finding was corroborated by electron microscopy showing the presence of ribosomes on spindles assembled from frog egg extracts. Taken together, these results suggest that protein translation occurs on the spindle during meiosis in the *Xenopus* oocyte. These findings were made possible due to the application of sequence-similarity methods, which extended mass spectrometric protein identification capabilities by 2-fold compared to conventional methods.

1 Introduction

Functional proteomics couples the purification of multiprotein complexes or organelles with the identification of their subunits by MS, thus providing an effective methodology for the elucidation of the molecular architecture of cells [1, 2]. Despite recent technological advances, relatively few species have been successfully explored at the proteome level, although existing evidence suggests that using a diversity of model organisms can broaden our knowledge of cell biology (reviewed in [3]). An important model organism in vertebrate biology that has not been amenable for functional proteomics is the African clawed frog *Xenopus laevis*. Research carried out on *Xenopus* oocytes and egg extracts has produced insights into the cell cycle [4], microtubule cytoskeleton regulation by microtubule-associated proteins (MAPs) [5], and spindle formation [6, 7]. Despite the importance of *X. laevis*, its large 3070 megabase pseudotetraploid genome [8] remains unsequenced, and the genome of the closely related species, *Xenopus tropicalis*, is planned to be sequenced by the DOE Joint Genome Institute by 2005, which significantly limits the rate at which isolated proteins can be identified.

Conventional techniques for MS-based protein identification rely strongly upon exact matching of masses of peptides and/or peptide fragments to corresponding masses calculated from sequences from database entries, and largely fail to identify proteins from organisms with unsequenced genomes. However, many proteins in different species are homologous, enabling proteins to be identi-

Correspondence: Dr. Andrej Shevchenko, Max Planck Institute of Molecular Cell Biology and Genetics, Pfotenhauerstrasse 108, D-01307 Dresden, Germany
E-mail: shevchenko@mpi-cbg.de,
Fax: +49-351-210-2000

---

† These authors contributed equally.
* Current address: Inserm Unité 366, DRDC/CS, CEA-Grenoble, F-38054 Grenoble, France
** Current address: Department of Physics, University of Manitoba, Winnipeg, R3T 2N2 Canada

fied by their sequence similarity to known homologues from phylogenetically related species. Here, we applied alternative MS data interpretation approaches (reviewed in [9]) and specialized database searching software [10, 11] to characterize the *Xenopus* microtubule associated proteome. Bioinformatic calculations presented here indicate that these techniques have wide phylogenetic applicability, and thus have a great potential to advance functional proteomics in many species.

2 Materials and methods

2.1 Purification of MAPs from *Xenopus* egg extract

CSF-arrested *Xenopus* egg extracts were prepared according to the method of A. Murray [4], frozen in liquid nitrogen in 200 µL PCR tubes, and stored at −80°C until use. We used 4 mL of extract *per* purification. The extract was thawed and diluted with two volumes of buffer BRB80 (80 mM K-piperazine-*N-N'*-bis-(2-ethanesulfonic acid), pH 6.8, 1 mM EGTA and 1 mM MgCl$_2$ and supplemented with 1 mM DTT, protease inhibitors and latrinkulin). To clarify the extract it was centrifuged twice for 15 min at 45 000 rpm in a Beckman TLA100.4 rotor (Palo Alto, CA, USA) at 4°C through a 1 mL cushion of BRB80 buffer with 40% glycerol. To assemble microtubules we used 4 mg pig brain tubulin, diluted to 8 mg/mL in BRB80 buffer and supplemented with 2 mM GTP. Microtubules were left to polymerize at 37°C for 30 min, further stabilized by addition of 20 µM taxol and pelleted at 50 000 rpm in the Beckman TLA100.2 rotor for 10 min at 20°C. Pelleted microtubules were resuspended in 0.5 mL BRB80/20 µM taxol and stored until use at room temperature. To bind MAPs and motors to microtubules the clarified extract was warmed to 20°C in a water bath and supplemented with 0.5 mL of prepolymerized microtubules assembled as described above, plus 1 mM GTP and 1.5 mM 5'-adenylylimidodiphosphate (AMPPNP). AMPPNP, a nonhydrolysable analogue of ATP, was shown to stabilize motors interaction with microtubules [12]. The extract was incubated with microtubules for 10 min at 20°C, overlaid onto a 1 mL BRB80 buffer/40% glycerol/20 µM taxol cushion and centrifuged for 10 min at 45 000 rpm in the Beckman TLA100.4 rotor at 20°C. Microtubule pellet was collected, resuspended in 3 mL of washing buffer (BRB80 buffer with 20 µM taxol, 1 mM DTT, 1 mM GTP) and centrifuged as above through a 1 mL BRB buffer/40% glycerol cushion. This step was repeated twice. The final pellet was taken up in 1 mL washing buffer containing 10 mM ATP for the elution of motor proteins. After a 10 min incubation at 20°C the microtubules were pelleted at 50 000 rpm in the Beckman TLA100.2 rotor for 10 min at 20°C, and the supernatant with eluted proteins (motor fraction) was transferred to ice.

The remaining microtubule pellet was taken up in 1 mL washing buffer supplemented with 0.5 mL NaCl, incubated at 20°C for 10 min and centrifuged through the glycerol cushion as described above. The supernatant with the MAPs fraction was collected and stored on ice until use or frozen in liquid nitrogen.

2.2 MS analysis

MAPs were resolved by 1-D polyacrylamide gel electrophoresis and stained with Coomassie. Protein bands were in-gel digested with trypsin (modified, sequencing grade; Promega, Madison, WI, USA) as previously described [13]. Collected peptides were first analyzed by peptide mass mapping on a Bruker Reflex IV MALDI TOF mass spectrometer (Bruker Daltonics, Leipzig, Germany) equipped with a Scout 384 ion source using AnchorChip™ targets 384/600 (Bruker Daltonics) as described [14]. Peptide mass maps were searched against the NCBI protein database (MSDB) using MASCOT v. 1.8 software [15] installed on a local server with mass tolerance of 150 ppm. No search parameters were imposed to limit species specificity for searches. Proteins not identified by peptide mass mapping were subjected to MS/MS analysis by nanoelectrospray on a hybrid quadrupole TOF mass spectrometer QSTAR™ Pulsar *i* (MDS Sciex, Concord, ON, Canada). All MS/MS spectra were first used for database searches with MASCOT at a mass tolerance of 0.1 Da for the precursor mass and 0.05 Da for fragment masses. Regardless of whether the confident protein identification was achieved by searches with MASCOT, MS/MS spectra were then searched with MS driven BLAST [10] at http://dove.embl-heidelberg.de/Blast2/msblast.html against a protein database (nrdb95), and then analyzed by MultiTag [11] (Table 1). For MS BLAST searches, BioAnalyst QS software (Applied Biosystems, Foster City, CA, USA) predicted *de novo* amino acid sequences with a tolerance of 0.1 Da for the precursor mass and 0.05 Da for fragment ion masses. The MS Blast processing script (version 1.1beta) automatically generated peptide sequences from MS/MS spectra and combined them in MS BLAST queries [16]. For MultiTag searches, sequence tags [17] were assembled by software-assisted interpretation of tandem mass spectra using BioAnalyst QS. Short (2–4 amino acid residues) stretches of peptide sequence were determined considering mass differences between abundant y-ions with *m/z* usually larger than the *m/z* of the precursor ion. Complete sequence tags (containing all three regions) were first searched against the NCBI protein nonredundant database (March 6, 2002) and the NCBI EST_others database (March 6, 2002) using PepSea database searching and subsequent MultiTag analysis as previously described [11].

Table 1. Identification of MAPs from *X. laevis*

No.	Peptide Mass Mapping-MASCOT	MS/MS-MASCOT	MS/MS-MS BLAST	MS/MS-MultiTag	MS BLAST	MultiTag		MultiTag in EST			
						TS	TM	Xe	EM	S	E-value
1. NaCl elution lane (Fig. 1A)											
1	Dynein heavy chain *R. norvegicus*, AAA41103										
2	XMAP 215kD *Xenopus*, CAB61894										
3	XMAP 215kD, *Xenopus*, CAB61894										
4				Glutamyl-prolyl-tRNA synthetase *H. sapiens*, XP_001958		11	5	41	1	1	1E-05
5		Bifunctional aminoa-cyl-tRNA-syn-thetase *H. sapiens*, P07814		Glutamyl-prolyl-tRNA synthetase *H. sapiens*, XP_001958		9	8	12	3	2	5E-08
6	XkIp1, *Xenopus*, I51617										
7	Isoleucyl-tRNA syn-thetase *PMF match to ATP 4**										
8				Hyaluronan mediated motility receptor, *Xenopus*(EST) BG363849		9	0	35	0	3	/
9				ISWI, *Xenopus*, AAG01537		12	4	29	5	2	1E-03
9				Eg5 , *Xenopus*, Q91783		12	3	29	13	2	1E-02
9				Leucyl-tRNA syn-thetase		12	4	29	0	0	/
10			DNA polymerase delta *H. sapiens*, P28340	DNA polymerase delta *H. sapiens*, S35455	3	12	7	31	1	1	8E-07
11			Kinesin heavy chain *Xenopus*, AJ249840	Kinesin 5B *M. musculus*, NP_032474	3	9	7	11	5	5	5E-08
12		Kinesin 5C *M. musculus,* AAC79804	Kinesin heavy chain *M. musculus*, L27153	Kinesin 5C *H. sapiens*, NP_004513	9	10	6	5	3	4	3E-08
13		Poly [ADP-ribose] polymerase *Xenopus*, P31735		Poly [ADP-ribose] polymerase *Xenopus*, P31669		11	8	88	5	2	1E-04

Table 1. Continued

No.	Peptide Mass Mapping-MASCOT	MS/MS-MASCOT	MS/MS-MS BLAST	MS/MS-MultiTag	MS BLAST	MultiTag		MultiTag in EST			
						TS	TM	Xe	EM	S	E-value
13			EMAP *H. sapiens*, Q9HC35	EMAP, **H. sapiens**, NP_061936	2	12	3	88	1	1	
14		Heat shock-like protein **M. musculus.** CAA34748	Heat shock protein 90-beta **S. salar**, AF135117	Heat shock protein 90-beta **D. rerio**, NP_571385	4	5	8	190	35	3	4E-09
14			Glutaminyl-tRNA synthetase **M. musculus**, AK003794	Glutaminyl-tRNA synthetase **H. sapiens**, NM_005051	2	8	7	190	14	8	6E-08
15	XNF7 *Xenopus*, AAB35876										
16	XNF7 *Xenopus*, AAB35876										
17	XNF7 *Xenopus*, AAB35877										
18	XkIp3A *Xenopus*, CAC33801										
19	Heat shock protein 70 *Xenopus*, AAB41583										
20				Lysyl-tRNA synthetase **H. sapiens**, BAA06688		9	9	71	21	4	1E-07
21			Formiminotransferase cyclo-deaminase **H. sapiens,** AF289023	Formiminotransferase Cyclodeaminase **S. scrofa**, P53603	3	12	2	172	8	4	2E-01
21		Tubulin alpha **G. mirabilis.** AAL24509		Tubulin alpha *Xenopus*, P08537		4	6	172	118	3	7E-10
22			Tubulin beta **H. sapiens**, BC020171	Tubulin beta-5 **G. gallus**, B27554	8	10	7	251	25	2	2E-07
22		Tubulin alpha 1 **H. sapiens**, AAH06468	Tubulin alpha **P. lividus**, A60671	Tubulin alpha *Xenopus*, CAA30093	5	7	12	251	137	7	2E-08
23	Tubulin beta-2 *Xenopus*, S05968										
24	Elongation factor gamma *Xenopus*, I51237										

Table 1. Continued

No.	Peptide Mass Mapping-MASCOT	MS/MS-MASCOT	MS/MS-MS BLAST	MS/MS-MultiTag	MS BLAST	MultiTag		MultiTag in EST			E-value
						TS	TM	Xe	EM	S	
25		Elongation factor 1-beta *Xenopus*, CAA49418	Elongation factor 1-beta *Xenopus*, P30151	Elongation factor 1-beta *Xenopus*, P30151	5	7	11	26	26	1	2E-08
26		Pancreatic trypsin inhibitor *B. taurus*, P00974	Pancreatic trypsin inhibitor *B. taurus*, X04666	Pancreatic trypsin inhibitor **B. taurus**, 1FAN	3	6	6	36	0	0	1E-08
2. ATP elution lane (Fig. 1B)											
1	Dynein heavy chain **R. norvegicus**, A38905										
2				Glutamyl-prolyl-tRNA synthetase **H. sapiens**, XP_001958		9	4	21	15	4	7E-07
3				Glutamyl-prolyl-tRNA synthetase **H. sapiens**, XP_001958		4	2	4	1	1	
4				Isoleucyl-tRNA synthetase **H. sapiens**, P41252		9	4	22	0	0	3E-05
5				Eg5, *Xenopus*, Q91783		7	2	6	1	1	
6		Kinesin heavy chain, **M. musculus**, AAC06326	Kinesin heavy chain **M. musculus,** X61435	Kinesin 5B **M. musculus**, NP_032474	2	8	6	3	1	3	1E-05
7	Kinesin heavy chain **H. sapiens**, A41919										
8		Elongation factor eEF-2 **R. norvegicus**, CAA68805		Elongation factor eEF-2 **C. elegans**, A40411		6	7	50	50	2	7E-07
9	Heat shock protein 90 **H. sapiens**, P07900										
10			Cytoplasmic dynein intermediate chain *Xenopus*, AF319781	Cytoplasmic dynein intermediate chain *Xenopus*, AF319781	3	9	10	63	17	5	6E-28
11		Heat shock protein 70.II *Xenopus*, AAB00199	Heat shock protein 68 **D. auraria**, AF247553	Heat shock protein 70 **P. olivaceus**, AAC33859	2	4	5	167	167	2	4E-09

Table 1. Continued

No.	Peptide Mass Mapping-MASCOT	MS/MS-MASCOT	MS/MS-MS BLAST	MS/MS-MultiTag	MS BLAST	MultiTag		MultiTag in EST			
						TS	TM	Xe	EM	S	E-value
12				Lysyl-tRNA synthetase ***H. sapiens***, Q15046		4	2	81	25	2	
13			HSP70/HSP90 organizing protein ***C. griseus***, AAB94760	HSP70/HSP90 organizing protein ***C. griseus***, AAB94760	3	7	4	25	13	2	7E-09
14	Elongation factor 1-gamma *Xenopus*, AAB29957	Elongation factor 1-gamma *Xenopus*, AAB29958	Elongation factor 1-gamma *Xenopus*, I51237	7	8	14	100	100	6	4E-08
14	Elongation factor 1-alpha *Xenopus*, CAA37169	Elongation factor 1-alpha *Xenopus*, P17507	Elongation factor 1-alpha *Xenopus*, P17508	8	11	10	95	95	5	8E-07
15	Elongation factor delta-2 *Xenopus*, S57631	Elongation factor 1-beta/delta ***C. elegans***, P34460	Elongation factor delta-2 *Xenopus*, S57631	2	5	7	46	46	3	2E-09
16				60S Ribosomal protein L5B *Xenopus*, P15126		5	3	66	39	2	2E-07
17	Ribosomal protein S3 ***M. musculus***, AAH10721	40S ribosomal protein S3 *Xenopus*, P47835	40S Ribosomal protein S3A *Xenopus*, P02350	1	7	4	120	20	2	9E-05
17	Activated protein kinase C receptor *Xenopus*, AAD42045		Activated protein kinase C receptor *Xenopus*, AAD42045		7	3	120	100	2	5E-03
18		Elongation factor 1-beta *Xenopus*, P30151	Elongation factor 1-beta *Xenopus*, P30151	5	5	9	70	70	5	3E-09
19	Pancreatic trypsin inhibitor *B. taurus*, P00974		Pancreatic trypsin inhibitor *B. taurus*, 1FAN		4	4	1	0	0	4E-07

3. Density gradient fractionation lane (Fig. 2)

No.	Peptide Mass Mapping-MASCOT	MS/MS-MASCOT	MS/MS-MS BLAST	MS/MS-MultiTag	MS BLAST	MultiTag		MultiTag in EST			
1	Dynein heavy chain ***R. norvegicus***, BAA02996										
2				Ataxia telangiectasia *Xenopus*, AAF20175		5	4	0	0	0	9E-11
3			Ataxia telangiectasia *Xenopus*, AAG40002		3						

Table 1. Continued

No.	Peptide Mass Mapping-MASCOT	MS/MS-MASCOT	MS/MS-MS BLAST	MS/MS-MultiTag	MS BLAST	MultiTag		MultiTag in EST			
						TS	TM	Xe	EM	S	E-value
4	Glutamyl-prolyl-tRNA synthetase *PMF match to ATP 2**			Glutamyl-prolyl-tRNA synthetase *Xenopus,* EST, BI443016		/	/	40	14	3	/
5	Isoleucyl-tRNA synthetase *PMF match to ATP 4**										
6		Leucyl-tRNA synthetase **H. sapiens**, BAA95667	Leucyl-tRNA synthetase **H. sapiens**, BAA95667	Leucyl-tRNA synthetase **H. sapiens**, BAA92590	8	7	4	/	/	/	8E-05
7	Glutaminyl-tRNA synthetase *PMF match to NaCl 14**										
8			Arginyl-tRNA synthetase **H. sapiens**, P54136	Arginyl-tRNA synthetase **T. elongatus**, NP_681615	9	7	3	/	/	/	3E-05
9	Lysyl-tRNA synthetase *PMF match to NaCl 20**										
10		Aspartyl-tRNA synthetase **H. sapiens,** AAH00629	Aspartyl-tRNA synthetase **H. sapiens**, P14868	Aspartyl-tRNA synthetase **H. sapiens,** P14868	6	5	9	/	/	/	3E-21

MAPs were identified by PMF and three types of searches with MS/MS spectra: nonerror tolerant searches with MASCOT and sequence similarity searches with MS BLAST and MultiTag. One protein (Leucyl tRNA synthetase, NaCl elution lane, band 9) was identified by matching tags to different database entries with the same functional identity. A few proteins (*) were identified by comparison of peptide mass map with better quality maps acquired from the corresponding bands in other lanes. Columns with identification data:
MS BLAST: no. of high scoring segment pairs for the hit; all identifications met MS BLAST statistical confidence criteria [18].
MutltiTag: no. of sequence tags submitted to the search (TS) and no. of tags matched to the hit (TM).
MultiTag in EST: no. of *Xenopus* ESTs retrieved from nonerror-tolerant searches (Xe), no. of *Xenopus* ESTs matching the top MultiTag hit (EM), no. of sequence tags matching *Xenopus* ESTs matched to the top MultiTag hit (S); E-values calculated for the top hit by MultiTag. In four cases, the identifications were not statistically confident (E-value > 1) and hits were validated by manual inspection of the spectra and by comparison with spectra obtained from the same protein confidently identified in other lanes. E-values were not provided in cases, where proteins were only identified in an EST database.

2.3 Density gradient fractionation

The motor fraction was prepared as described in Section 2.1. Proteins were eluted in 1 mL of 20 mM ATP and concentrated by centrifugation on Millipore biomax filters (cutoff size 10 kDa; Bedford, MA, USA) to 100 μL before loading them onto continuous 5–45% sucrose gradients prepared in SW60 Beckman tubes. Sucrose gradients were centrifuged for 9 h at 37 000 rpm at 4°C and 200 μL fractions were collected manually from the top of the tub and analyzed by electrophoresis on 6–20% polyacrylamide gradient gels.

2.4 Spindle assembly and electron microscopy

Spindle assembly was performed according to the method of A. Desai (personal communication, Ludwig Institute for Cancer Research at UCSD, La Jolla, CA, USA). Seven

minutes after the addition of 0.4 mM CaCl$_2$ at 20°C, 20 µL of the anaphase spindle assembly mixture was added to 1 mL of the dilution buffer (30% glycerol in BRB80 buffer), and fixed by the addition of 1 mL of 50 mM lysine, 3% gluteraldehyde in BRB80 buffer for 10 min at room temperature. The sample was layered over 4 mL of cushion (30% glycerol in BRB80 buffer) in a tube with glow discharged, poly-L-lysine coated Aclar coverslip on chock, and pelleted at 5500 rpm in the HS4 Beckman rotor at 16°C for 20 min. The tube walls were washed with BRB80 buffer, and aspirated down to a minimal fluid covering the coverslip. The coverslip was withdrawn, rinsed in BRB80 buffer, placed in a humidified chamber and fixed with 1.5% gluteraldehyde in BRB80 buffer for 10 min. It was then rinsed with BRB80 buffer, 0.05 M cacodylate buffer at pH 7.0, and postfixed with 1% osmium in 0.8% K$_3$Fe (CN)$_6$ in cacodylate for 15 min on ice, and finally rinsed again with cacodylate. The coverslip was stained overnight in 1% aqueous uranyl acetate at 4°C in the dark and then rinsed and dehydrated in neat ethanol by progressive lowering of the temperature to −40°C. The sample was brought to room temperature and dipped in fresh ethanol, then in neat propylene oxide, and then infiltrated with propylene oxide:epon araldite (2:1, 1:2), 100% epon araldite for 1 h *per* step. It was mounted and left to polymerize at 65°C for 48 h. Spindles were selected and serially thin sectioned with a Druuker DMK (Druuker, Cuijk, The Netherlands) diamond knife on a Reichert Ultracut S (Reichert, Vienna, Austria). They were stained, viewed and imaged on a JEOL 1200 electron microscope (JEOL, Peabody, MA, USA).

2.5 Computing MS driven BLAST specificity and phylogenetic distances

MS BLAST searches were carried out for 1000 proteins from several model organisms (*Saccharomyces cerevisiae*, *Schizosaccharomyces pombe*, *Candida albicans*, *Takifuga rubripes*, *Rattus norvegicus*, *Mus musculus* and *Homo sapiens*) as described in [18]. To estimate the success of MS BLAST searches, queries comprised of 10 peptide sequences were used. Each peptide was 10 amino acids in length with two randomly inserted zero scoring X residues to simulate ambiguities in the interpretation of tandem mass spectra. Statistically significant hits of MS BLAST searches were collected and tested for positive or negative identification by BLAST searches with the full length sequence of proteins, from which MS BLAST queries were assembled. A phylogenetic tree of organisms from three subkingdoms was constructed based on mitochondrial small subunit ribosomal RNAs. Multiple sequence alignments were made using the program ClustalX [19], and the phylogenetic trees were constructed with the

programs dnadist and fitch, both from the Phylip package (J. Felsenstein, distributed by the author). The estimated success rate of MS BLAST identifications was correlated with phylogenetic distances between a model set of organisms [18] and was applied to a larger set of organisms on the phylogenetic tree.

3 Results and discussion

3.1 MS analysis of microtubule-associated proteins

Proteins were isolated from *X. laevis* egg extracts through binding and subsequent elution from microtubules using ATP or salt. The eluted proteins were resolved by 1-D polyacrylamide gel electrophoresis, and identified by MS. We first screened for proteins with a high degree of sequence similarity compared to available database sequences using PMF. Proteins not identified by PMF were subjected to MS/MS analysis. The conventional MS/MS spectra analysis and database searching software compares lists of observed fragment masses with predicted fragment ion masses to identify peptides that are highly similar to database entries [20]. If a close homologue of the analyzed protein is not present in a database, conventional protein identification methods fail. In these cases, sequence-similarity approaches were used to identify homologous proteins beyond the limits of the conventional software. Of the two sequence-similarity methods applied, MS BLAST [10] requires that amino acid sequences be predicted *de novo* from tandem mass spectra and used as a query in a database search. A combination of many, possibly low confidence, predictions can be used as a query for the database search, although with specific options and a different statistical consideration. Where confident *de novo* sequence prediction is not possible, the MultiTag approach can identify proteins from noisy and low intensity spectra. MultiTag makes use of a few (typically, from two to four) correctly identified amino acid residues *per* peptide that are assembled in a format of the sequence tag [17] for the protein identification. Peptide sequence tags determined by the interpretation of tandem mass spectra acquired from several precursor ions are used in multiple degenerate error tolerant database searches [11]. MultiTag further computes the statistical significance of multiple error tolerant matches to the same protein sequence, and thus pinpoints database proteins homologous to the query.

Both MS BLAST and MultiTag estimate the statistical probability that a given combination of peptide sequences or sequence tags will hit a database entry at random. Confident protein identification can, in principle, be achieved by a single error tolerantly matching peptide

or tag. Although no penalty is explicitly imposed for non-matched sequences or tags, the overall confidence decreases with the size of the query, because of the increased probability of producing a random hit from a larger number of possible combinations. Therefore error tolerant searching (regardless of the statistical method applied) is not well suited to a shotgun approach [21], however, it is relatively straightforward to dissect simple mixtures comprising up to 10 unknown proteins. From three gel lanes, 55 protein bands were analyzed and 61 proteins were identified (Figs. 1 and 2). The conventional software identified 20 proteins by PMF and 19 proteins from MS/MS spectra. From the same set of MS/MS

spectra, sequence-similarity database searching by MS BLAST identified 24 proteins and MultiTag identified 41 proteins (this included all of the proteins identified by the conventional software and MS BLAST but one, plus 17 more) (Table 1). Proteins were identified using *Xenopus* database entries, making 29 determinations, and 32 proteins were identified by cross-species reference to homologous sequences from *Homo sapiens*, *Mus musculus*, *Rattus norvegicus*, *Cricetulus griseus*, *Sus scrofa*, *Gallus gallus*, *Gillichthys mirabilis*, *Paralichthys olivaceus*, *Salmo salar*, *Danio rerio*, *Paracentrotus lividus*, *Caenorhabditis elegans*, *Drosophila auraria,* and *Thermosynechococcus elongatus*.
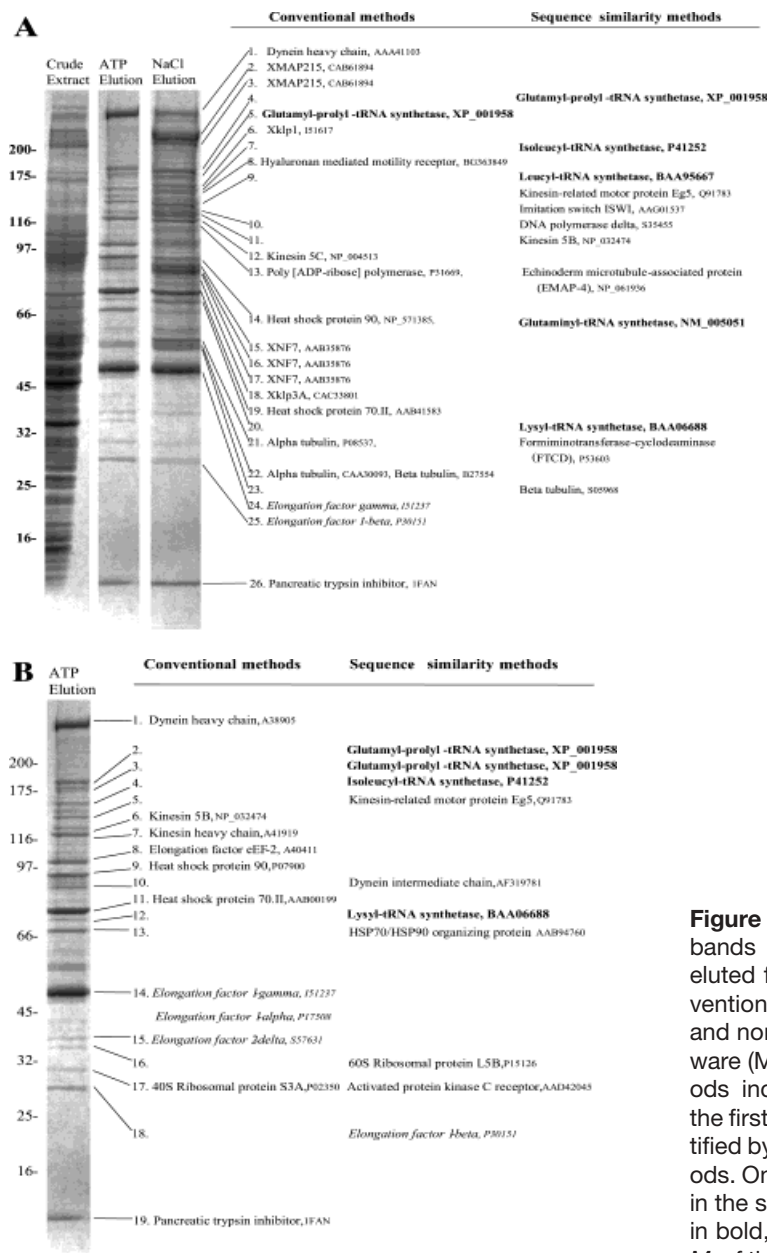

Figure 1. Identification of MAPs. The analysis of protein bands by in-gel digestion and MS identified proteins eluted from microtubules by NaCl (A) and ATP (B). Conventional protein identification methods included PMF and nonerror tolerant MS/MS spectra interpretation software (MASCOT). Sequence similarity identification methods included MS BLAST and MultiTag. All proteins in the first column that were identified by MS/MS were identified by both conventional and sequence similarity methods. Only sequence similarity methods identified proteins in the second column. Members of the ARS complex are in bold, members of the EF-1 complex are in italics. The M_r of the markers is presented in kDa.

Although a sizable amount of *X. laevis* ESTs are available [22], we found that EST database searching alone was insufficient for facile protein identification. Where ESTs could be retrieved from the interpretation of MS/MS spectra with sequence tags and database searching, it was difficult to determine which of the multiple retrieved ESTs coded for the analyzed protein (without manual inspection of hundreds of retrieved EST matches), due to the degenerate nature of the sequence tag database search. In our study, only one protein was identified by EST database searching alone, which was not found by searching a protein database (Table 1).

The identified proteins can be grouped in three classes: (1) previously described MAPs and motors, (2) proteins reported to be associated with the microtubule cytoskeleton, but without a clearly defined cytoskeletal function (like heat shock proteins (HSPs)), and (3) proteins not previously described as having microtubule localization (Table 2). In the first and second groups, we identified several known kinesins as well as dynein heavy and intermediate chains, and four previously characterized MAPs. Among the proteins of the third group we detected components of two multiprotein complexes. These are: four subunits of the 750 kDa guanine nucleotide exchange EF-1βγδ complex [23], and seven aminoacyl-tRNA synthetases (ARSs) known to form a multisubunit complex thought to exist in all higher eukaryotes [24]. The ARS complex has been shown to consist of eight to nine ARSs and three nonsynthetase components. The ARS complex is essential for aminoacylation of tRNAs prior to polypeptide synthesis (reviewed in [24]) and the EF-1 complex exchanges GTP/GDP in the binding and transportation of aminoacyl-tRNAs to the ribosome [23].

3.2 Association of the ARS complex with microtubules

A physical interaction of the ARS complex with microtubules in meiosis has not been observed previously. We reasoned that the complex might be either directly bound to microtubules, or might represent a cargo complex tethered to microtubules *via* a motor protein. Indeed, the ARS complex was eluted from microtubules with excess ATP, along with other kinesin proteins whose association is known to be ATP-dependent. Accidental copelleting of the ARS complex with microtubules is excluded, since the complex was recovered not in the pellet, but in the supernatant only after the addition of ATP. Furthermore, ATP added to the egg extract prior to mixing with microtubules also prevented the ARS complex from binding to microtubules (data not shown). We therefore concluded that binding of the ARS complex to microtubules is specific and ATP-sensitive.
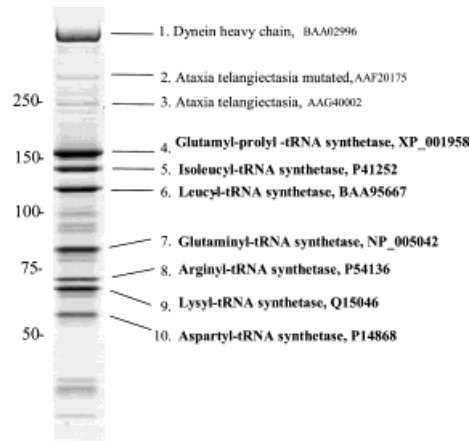

Figure 2. Purification of the ARS complex. Microtubule-bound proteins were eluted by ATP and further fractionated on a sucrose density gradient, with one unique fraction corresponding to *ca.* 15 S shown above. Seven ARSs were coisolated on the sucrose density gradient fractionation. Members of the ARS complex are in bold.

We further examined if the ARS could be a cargo complex, associated with microtubules *via* a motor protein. ATP-eluted proteins were fractionated on a sucrose density gradient and resolved by gel electrophoresis. We identified a fraction that included seven ARSs and dynein heavy chain (Fig. 2). Whereas five lanes contained this pattern, one lane contained only the ARS complex but no dynein heavy chain (data not shown), suggesting their independent binding to microtubules. As p50 (dynamitin) disrupts the dynein/dynactin interaction *in vivo* and *in vitro* [25], we examined whether p50 would dissociate the ARS complex from microtubules in the presence of dynein. After p50 addition, some proteins like Xenopus nuclear factor 7 disappeared from the microtubule pellet, but we still detected ARSs in the bound fraction by MS/MS (data not shown). These experiments suggested that the ARS complex is not a classical dynein/dynactin cargo. Since MS analysis of other, minor protein bands present in the ARS containing fraction did not detect any other motor proteins, we concluded that the ARS complex is attached to microtubules directly.

3.3 *In vitro* spindle reconstitution and electron microscopy

We have demonstrated that two essential components of the protein translation machinery, the EF-1 complex and the ARS complex are bound to microtubules in meiotic egg extracts. These findings suggested that protein translation may be spatially connected with the spindle. To verify this hypothesis, we assembled spindles in *Xenopus* egg extracts and imaged them by electron micros-
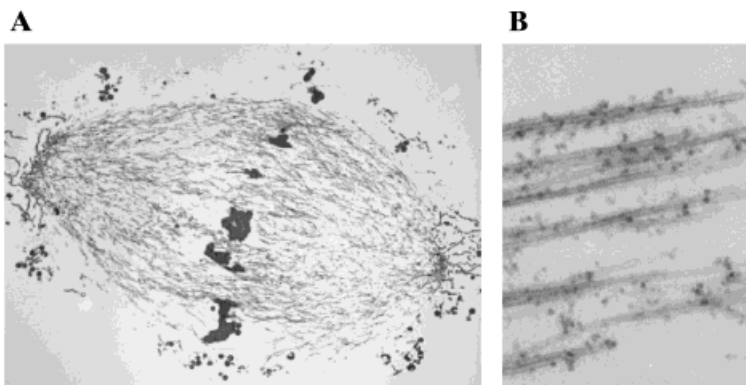
Figure 3

A   B

Figure 3. Electron microscopy images of the *Xenopus* spindle reconstituted *in vitro*. (A) Initial low magnification images show ribosomes in clusters located peripheral to the centrosomes. (B) Upon higher magnification, ribosomes were found to be distributed along the length of the spindle microtubules.

copy. Remarkably, we detected ribosomes, that appeared in clusters located peripheral to the centrosomes (Fig. 3A) and were distributed along the length of the spindle microtubules (Fig. 3B), further suggesting that the protein translation machinery is localized on the spindle *in vivo*.

3.4 Implications of *Xenopus* proteomics

Due to the large size of *Xenopus* oocytes and the fact that they contain an abundance of cytoplasmic proteins necessary for early development, these cells or extracts prepared from them have been the preferred model system for the study of the mitotic spindle and spindle associated proteins [6]. Additionally, MAPs have been analyzed by purification and MS in other organisms, such as human, *Drosophila*, and yeast. However, from the sixteen microtubule-bound proteins purified by Mack and Compton in 2001 from mitotic HeLa cells, only two (Eg5 and HSP70) are on the list of proteins identified by us [26]. In a systematic analysis of centrosome-associated proteins (many MAPs are also centrosomal components, see [27]) from *Drosophila*, only one identified protein was also found in our preparation (HSP90) [28]. Similarly, of the eight proteins identified by Adams and Kilmartin [29] from *S. cerevisiae* spindle pole bodies, none matched those found in our preparation. In a recent study of human centrosomal proteins, Andersen *et al.* [30] identified altogether 47 known centrosomal proteins and 23 proteins were new. Among *bona fide* centrosomal proteins, only four matched those on our list of MAPs and proteins with known cytoskeleton localization (Table 2). Interestingly, in their centrosome preparation Andersen *et al.* identified many known components of the translation machinery, including three out of seven ARSs, which form the ARS complex and three additional ARSs. They also identified

components of EF1 and EF2 complexes, as well as both ribosomal proteins listed in Table 2. Thus the comparative analysis of identified MAPs underscores the importance of a multiorganismal approach in the proteomic characterization of the cytoskeleton.

The finding that the ARS complex and the EF-1 complex of the protein translation machinery were bound to microtubules in egg extracts, and electron microscopy images showing the abundance of ribosomes on the reconstituted spindle, prompted speculations about the potential existence of such interactions *in vivo*. The ARS and EF-1 complexes were identified primarily in the ATP-elution samples and, interestingly, there is evidence that they may interact with each other *in vitro* [31]. Although we did not probe the direct association of ribosomes with other proteins identified by us, it is known that ribosomes are associated *in vivo* with both elongation factors and ARS and can be even used for their affinity purification *in vitro* [32].

Our results suggest that protein translation during meiosis occurs on spindle microtubules. Indeed, ribosomes have also been found previously on microtubules isolated from unfertilized sea urchin eggs, and their attachment was mediated through another protein found in our screen (EMAP) [33]. Spatial regulation of translation could be especially important for large cells like *Xenopus* oocytes. Although transcription of cyclin B1 [34] occurs during mitosis, protein synthesis has not been directly detected in mitotic cells. On the contrary, *de novo* synthesis of several cell cycle components, including c-mos, cyclin B1, and XKID is essential during meiosis [35, 36]. Furthermore, cyclin B1 mRNA was found associated with meiotic spindles and it was suggested that translation of cyclin B1 occurs locally, on or near spindles and centrosomes [37]. Our findings lend further support to this interpretation.
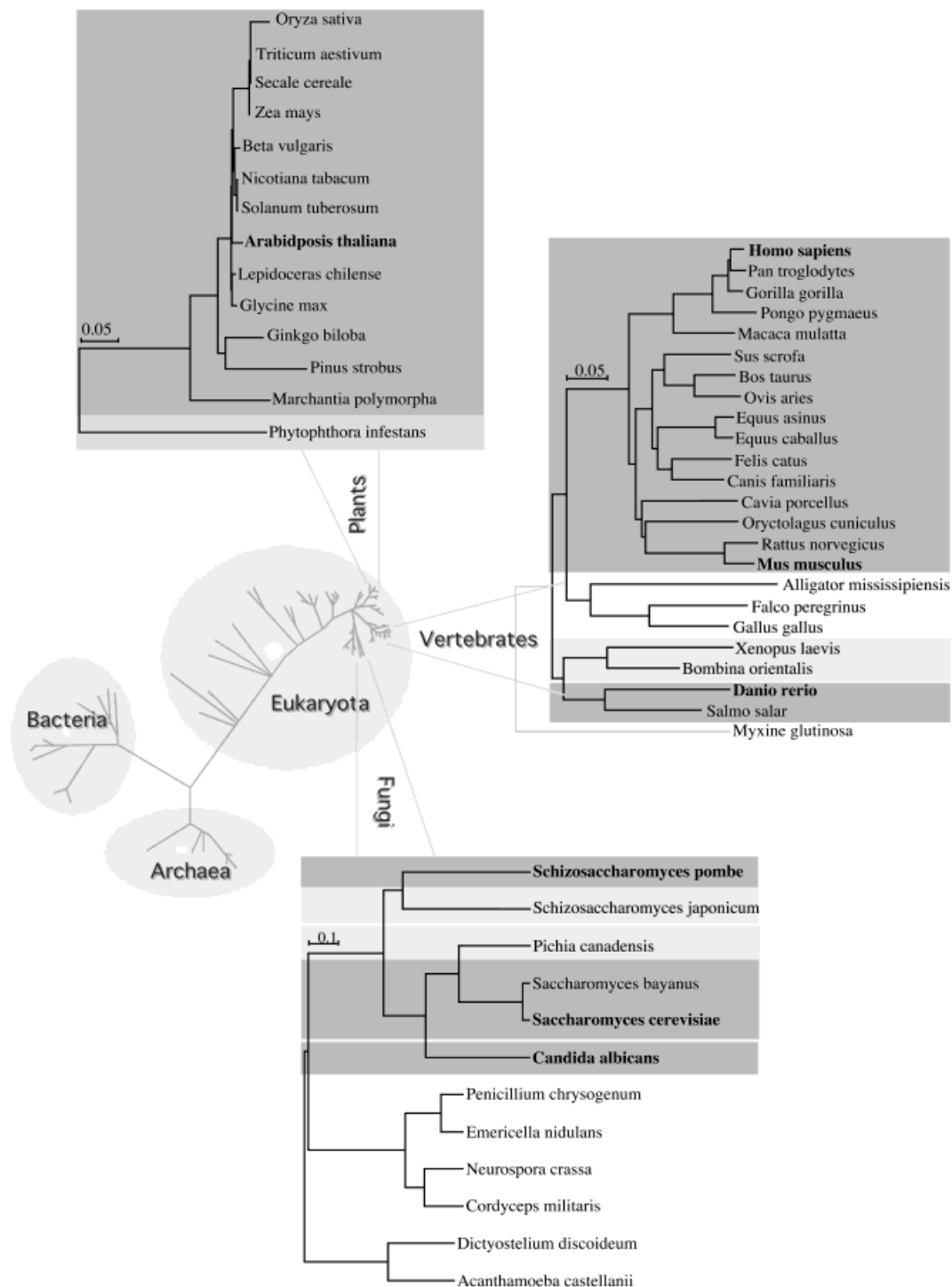
Figure 4. Computational evaluation of the success of protein identification by sequence-similarity searches in organisms with unsequenced genomes. Three partial phylogenetic trees of major subkingdoms branch from a phylogenetic tree of all living organisms. Phylogenetic analysis was used to estimate the success of proteome characterization by MS and sequence-similarity database searching, based on the specificity of MS BLAST to identify homologous proteins. For organisms in the area highlighted with dark grey the expected MS BLAST coverage of unknown proteomes exceeds 90%; with middle grey: between 30 and 50%; with light grey: lower than 30% coverage. Reference organisms with sequenced genomes are typeset in bold. The scale bar reflects the number of nucleotide substitutions *per* site.

Table 2. Functional categories of proteins identified in the microtubule-bound fractions

	Protein	Localization/function	Identification
(1) MAPs and motor proteins			
1	Dynein heavy chain	ATPase domain-containing chain of the dynein complex [38]	*x-species*
2	XMAP310	Unknown function [39]	AB
3	XMAP230	Unknown function [40]	AB
4	XMAP215	Microtubule-associated protein, regulation of microtubule dynamics [41]	*Xenopus,* AB
5	Xklp1	Chromokinesin [42]	*Xenopus*
6	Eg5	Plus-end-directed microtubule motor [43, 44]	*Xenopus*
7	Kinesin 5B	Kinesin heavy chain member 5B [45]	*x-species*
8	Kinesin 5C	Neuron-specific kinesin heavy chain member 5C [46]	*x-species*
9	EMAP4	a WD repeat protein, localizes to microtubules and promotes microtubule dynamics [47]	*x-species*
10	Xklp3	Kinesin II motor protein [48]	*Xenopus*
11	Xklp3A	Kinesin II motor protein [48]	*Xenopus*
12	Dynein intermediate chain	Part of the dynein minus-end motor complex [49]	*Xenopus.*
13	Alfa tubulin	Part of the alpha-beta tubulin dimer [50]	*x-species, Xenopus*
14	Beta tubulin	Part of the alpha-beta tubulin dimer [51]	*x-species, Xenopus*
(2) Proteins with previously described microtubule cytoskeleton localization			
1	RHAMM, (Hyaluronan mediated motility receptor)	RHAMM was reported to be associated with microtubuless in interphase and mitotic cells as well as with microtubules in vitro [52]	*Xenopus*
2	ISWI (imitation switch protein)	ATP-dependent chromatin-remodeling factor [53, 54]	*Xenopus*
3	Poly (ADP-ribose) polymerase (PARP)	Telomeres, mitotic centrosomes [55]	*Xenopus*
4	Heat shock protein 90	Localizes to microtubules, centrosome [28, 56]	*x-species*
5	Heat shock protein 70.II	Localizes to microtubules [56]	*Xenopus*
6	XNF7	Xenopus nuclear factor 7, protein with function in dorsal/ventral patterning of the embryo. In mitosis localizes to mitotic spindle [57]	*Xenopus*
7	FTCD	Formininotransferase cyclodeaminase, microtubule-binding Golgi protein [58]	*x-species*
(3) Proteins not previously described as having microtubule localization			
1	Ataxia telangiectasia protein	Chromatin-binding protein [59]	*Xenopus*
2	Ataxia telangiectasia protein	Chromatin-binding protein [60]	*Xenopus*
3	Glutamyl-prolyl-bifunctional aminoacyl tRNA synthetase	Part of a multicomponent aminoacyl-tRNA synthetase complex [24]	*x-species*
4	Isoleucyl-tRNA synthetase	Part of a multicomponent aminoacyl-tRNA synthetase complex [24]	*x-species*
5	Leucyl-tRNA synthetase	Part of a multicomponent aminoacyl-tRNA synthetase complex [24]	*x-species*
6	DNA-polymerase delta, catalytic subunit	Part of the three-subunit DNA polymerase delta [60]	*x-species*
7	eEF-2	Translation elongation factor [61]	*x-species*
8	Glutaminyl-tRNA synthetase	Part of a multicomponent aminoacyl-tRNA synthetase complex [24]	*x-species*
9	Arginyl-tRNA synthetase	Part of a multicomponent aminoacyl-tRNA synthetase complex [24]	*x-species*
10	Lysyl-tRNA synthetase	Part of a multicomponent aminoacyl-tRNA synthetase complex [24]	*x-species*
11	HSP70/HSP90 organizing protein	Stress-response protein [62]	*Xenopus*
12	Aspartyl-tRNA synthetase	Part of a multicomponent aminoacyl-tRNA synthetase complex [24]	*x-species*

Table 2. Continued

	Protein	Localization/function	Identification
13	EF 1-gamma	Beta, delta and gamma subunits of EF1 form a guanine nucleotide exchange complex (co-localize with the endoplasmic reticulum) [23]	*Xenopus*
14	EF 1-alpha	Substrate of the guanine-nucleotide exchange complex [23]	*Xenopus*
15	EF 1-delta-2	Homologous to the EF-delta-1, part of the guanine-nucleotide exchange complex of elongation factor-1 (EF-1) [23]	*Xenopus*
16	60S Ribosomal protein L5B	60S subunit ribosome-binding protein. Was previously described in association with the ARS complex [63]	*Xenopus*
17	40S Ribosomal protein S3A	40S ribosomal subunit [64]	*Xenopus*
18	Activated protein kinase C receptor (RACK1)	Highly conserved WD protein expressed during embryogenesis [65]	*Xenopus*
19	EF 1-beta	Part of the guanine nucleotide exchange complex of EF-1 [23]	*Xenopus*

Identified proteins are grouped into three categories according to their proposed function (see Section 3.1). Proteins were identified by MS and referenced to *X. laevis* database sequences (*Xenopus*) or cross-species referenced to sequences other than *Xenopus* (*x-species*). Alpha- and beta-tubulin monomers were identified with *Xenopus* and other species entries, for example pig tubulins. Additional identifications were made by immunoblot analysis using specific antibodies (AB).

4 Concluding remarks

Our findings demonstrate the power of sequence-similarity protein identification methods combined with cell biological approaches for the functional proteomics of organisms beyond the boundaries of sequenced genomes. To evaluate the success of proteome characterization in organisms with unsequenced genomes, we estimated by computational modeling the specificity of MS BLAST to identify homologous proteins in species of various phylogenetic lineages [18]. The success rate of MS BLAST searches was correlated to the phylogenetic distance of the organism under study to the closest organism with a fully sequenced genome. With the analysis of 10 peptides (each 10 amino acids in length, with two undetermined residues placed at randomly chosen positions in their sequence), MS BLAST could successfully identify the majority of proteins down to a limit of 65% sequence identity to their closest homologues in a database. Taking into consideration eight species with sequenced genomes, we proposed groups of species, in which sequence-similarity methods would be effective (Fig. 4). With these developments, functional proteomics in important model species with unsequenced genomes has the potential to be advanced by MS and sequence-similarity database searching.

5 References

[1] Dreger, M., *Eur. J. Biochem.* 2003, *270*, 589–599.

[2] Jung, E., Heller, M., Sanchez, J. C., Hochstrasser, D. F., *Electrophoresis* 2000, *21*, 3369–3377.

[3] Liska, A. J., Shevchenko, A., *Proteomics* 2003, *3*, 19–28.

[4] Murray, A. W., Kirschner, M. W., *Nature* 1989, *339*, 275–280.

[5] Cassimeris, L., Spittle, C., *Int. Rev. Cytol.* 2001, *210*, 163–226.

[6] Karsenti, E., Vernos, I., *Science* 2001, *294*, 543–547.

[7] Lohka, M. J., Maller, J. L., *J. Cell Biol.* 1985, *101*, 518–523.

[8] Graf, J. D., Kobel, H. R., *Methods Cell. Biol.* 1991, *36*, 19–34.

[9] Liska, A. J., Shevchenko, A., *Trends Anal. Chem.* 2003, *22*, 291–298.

[10] Shevchenko, A., Sunyaev, S., Loboda, A., Shevchenko, A. *et al.*, *Anal. Chem.* 2001, *73*, 1917–1926.

[11] Sunyaev, S., Liska, A. J., Golod, A., Shevchenko, A. *et al.*, *Anal. Chem.* 2003, *75*, 1307–1315.

[12] Lasek, R. J., Brady, S. T., *Nature* 1985, *316*, 645–647.

[13] Shevchenko, A., Wilm, M., Vorm, O., Mann, M., *Anal. Chem.* 1996, *68*, 850–858.

[14] Thomas, H., Havlis, J., Peychl, J., Shevchenko, A., *Rapid Commun. Mass Spectrom.* 2004, *18*, *in press*.

[15] Perkins, D. N., Pappin, D. J., Creasy, D. M., Cottrell, J. S., *Electrophoresis* 1999, *20*, 3551–3567.

[16] Shevchenko, A., Sunyaev, S., Liska, A., Bork, P. *et al.*, *Meth. Mol. Biol.* 2002, *211*, 221–234.

[17] Mann, M., Wilm, M., *Anal. Chem.* 1994, *66*, 4390–4399.

[18] Habermann, B., Oegema, J., Sunyaev, S., Shevchenko, A., *Mol. Cell. Proteomics* 2004, *3*, 238–249.

[19] Thompson, J. D., Gibson, T. J., Plewniak, F., Jeanmougin, F. *et al.*, *Nucleic Acids Res.* 1997, *25*, 4876–4882.

[20] Creasy, D. M., Cottrell, J. S., *Proteomics* 2002, *2*, 1426–1434.

[21] Washburn, M. P., Wolters, D., Yates, J. R. 3rd., *Nat. Biotechnol.* 2001, *19*, 242–247.

[22] Blackshear, P. J., Lai, W. S., Thorn, J. M., Kennington, E. A. *et al.*, *Gene* 2001, *267*, 71–87.

[23] Minella, O., Mulner-Lorillon, O., Poulhe, R., Belle, R. *et al.*, *Eur. J. Biochem.* 1996, *237*, 685–690.

[24] Ibba, M., Soll, D., *Annu. Rev. Biochem.* 2000, *69*, 617–650.

[25] Wittmann, T., Hyman, T., *Methods Cell. Biol.* 1999, *61*, 137–143.

[26] Mack, G. J., Compton, D. A., *Proc. Natl. Acad. Sci. USA* 2001, *98*, 14434–14439.

[27] Popov, A. V., Severin, F., Karsenti, E., *Curr. Biol.* 2002, *12*, 1326–1330.

[28] Lange, B. M., Bachi, A., Wilm, M., Gonzalez, C., *EMBO J.* 2000, *19*, 1252–1262.

[29] Adams, I. R., Kilmartin, J. V., *J. Cell Biol.* 1999, *145*, 809–823.

[30] Andersen, J. S., Wilkinson, C. J., Mayor, T., Mortensen, P. *et al.*, *Nature* 2003, *426*, 570–574.

[31] Sang Lee, J., Gyu Park, S., Park, H., Seol, W. *et al.*, *Biochem. Biophys. Res. Commun.* 2002, *291*, 158–164.

[32] Ganoza, M. C., Aoki, H., Burkhardt, N., Murphy, B. J., *Biochimie* 1996, *78*, 51–61.

[33] Suprenant, K. A., Tempero, L. B., Hammer, L. E., *Cell Motil. Cytoskeleton* 1989, *14*, 401–415.

[34] Sciortino, S., Gurtner, A., Manni, I., Fontemaggi, G. *et al.*, *EMBO Rep.* 2001, *2*, 1018–1023.

[35] Hochegger, H., Klotzbucher, A., Kirk, J., Howell, M. *et al.*, *Development* 2001, *128*, 3795–3807.

[36] Perez, L. H., Antonio, C., Flament, S., Vernos, I. *et al.*, *Nat. Cell Biol.* 2002, *4*, 737–742.

[37] Groisman, I., Huang, Y. S., Mendez, R., Cao, Q. *et al.*, *Cell* 2000, *103*, 435–447.

[38] Mikami, A., Paschal, B. M., Mazumdar, M., Vallee, R. B., *Neuron* 1993, *10*, 787–796.

[39] Andersen, S. S., Karsenti, E., *J. Cell Biol.* 1997, *139*, 975–983.

[40] Andersen, S. S., Buendia, B., Dominguez, J. E., Sawyer, A. *et al.*, *J. Cell Biol.* 1994, *127*, 1289–1299.

[41] Tournebize, R., Popov, A., Kinoshita, K., Ashford, A. J. *et al.*, *Nat. Cell Biol.* 2000, *2*, 13–19.

[42] Vernos, I., Heasman, J., Wylie, C., *Dev. Biol.* 1993, *157*, 232–239.

[43] Houliston, E., Le Guellec, R., Kress, M., Philippe, M. *et al.*, *Dev. Biol.* 1994, *164*, 147–159.

[44] Sawin, K. E., LeGuellec, K., Philippe, M., Mitchison, T. J., *Nature* 1992, *359*, 540–543.

[45] Gudkov, A. V., Kazarov, A. R., Thimmapaya, R., Axenovich, S. A. *et al.*, *Proc. Natl. Acad. Sci. USA* 1994, *91*, 3744–3748.

[46] Nagase, T., Ishikawa, K., Miyajima, N., Tanaka, A. *et al.*, *DNA Res.* 1998, *5*, 31–39.

[47] Hamill, D. R., Howell, B., Cassimeris, L., Suprenant, K. A., *J. Biol. Chem.* 1998, *273*, 9285–9291.

[48] De Marco, V., Burkhard, P., Le Bot, N., Vernos, I. *et al.*, *EMBO J.* 2001, *20*, 3370–3379.

[49] Zhang, J., Han, G., Xiang, X., *Mol. Microbiol.* 2002, *44*, 381–392.

[50] Smith, D. J., *Biochem. J.* 1988, *249*, 465–472.

[51] Good, P. J., Richter, K., Dawid, I. B., *Nucleic Acids Res.* 1989, *17*, 8000.

[52] Assmann, V., Jenkinson, D., Marshall, J. F., Hart, I. R., *J. Cell Sci.* 1999, *112*, 3943–3954.

[53] Tsukiyama, T., Palmer, J., Landel, C. C., Shiloach, J. *et al.*, *Genes Dev.* 1999, *13*, 686–697.

[54] Trachtulcova, P., Janatova, I., Kohlwein, S. D., Hasek, J., *Yeast* 2000, *16*, 35–47.

[55] Earle, E., Saxena, A., MacDonald, A., Hudson, D. F. *et al.*, *Hum. Mol. Genet.* 2000, *9*, 187–194.

[56] Liang, P., MacRae, T. H., *J. Cell Sci.* 1997, *110*, 1431–1440.

[57] Etkin, L. D., el-Hodiri, H. M., Nakamura, H., Wu, C. F. *et al.*, *J. Cell. Physiol.* 1997, *173*, 144–146.

[58] Bashour, A. M., Bloom, G. S., *J. Biol. Chem.* 1998, *273*, 19612–19617.

[59] Robertson, K., Hensey, C., Gautier, J., *Oncogene* 1999, *18*, 7070–7079.

[60] Chung, D. W., Zhang, J. A., Tan, C. K., Davie, E. W. *et al.*, *Proc. Natl. Acad. Sci. USA* 1991, *88*, 11197–11201.

[61] Ofulue, E. N., Candido, E. P., *DNA Cell Biol.* 1991, *10*, 603–611.

[62] Heine, H., Delude, R. L., Monks, B. G., Espevik, T. *et al.*, *J. Biol. Chem.* 1999, *274*, 21049–21055.

[63] Wormington, W. M., *Mol. Cell. Biol.* 1989, *9*, 5281–5288.

[64] Amaldi, F., Beccari, E., Bozzoni, I., Luo, Z. X. *et al.*, *Gene* 1982, *17*, 311–316.

[65] Kwon, H. J., Bae, S., Son, Y. H., Chung, H. M., *Dev. Genes Evol.* 2001, *211*, 195–197.